

Phase-matching enhanced quantum phase and amplitude estimation of a two-level system in a squeezed reservoir

Yan-Ling Li(李艳玲), Cai-Hong Liao(廖彩红), and Xing Xiao(肖兴)

Citation: Chin. Phys. B, 2025, 34 (**1**): 010307. DOI: 10.1088/1674-1056/ad8f9e
Journal homepage: http://cpb.iphy.ac.cn; http://iopscience.iop.org/cpb

What follows is a list of articles you may be interested in

Parameter estimation in *n*-dimensional massless scalar field

Ying Yang(杨颖) and Jiliang Jing(荆继良)
Chin. Phys. B, 2024, 33 (**3**): 030307. DOI: 10.1088/1674-1056/ad1749

Holevo bound independent of weight matrices for estimating two parameters of a qubit

Chang Niu(牛畅) and Sixia Yu(郁司夏)
Chin. Phys. B, 2024, 33 (**2**): 020304. DOI: 10.1088/1674-1056/ad117d

Compact generation scheme of path-frequency hyperentangled photons using 2D periodical nonlinear photonic crystal

Yang-He Chen(陈洋河), Bo Ji(季波), Nian-Qin Li(李念芹), Zhen Jiang(姜震), Wei Li(李维),Yu-Dong Li(李昱东), Liang-Sen Feng(冯梁森), Teng-Fei Wu(武腾飞), and Guang-Qiang He(何广强)
Chin. Phys. B, 2023, 32 (**12**): 120307. DOI: 10.1088/1674-1056/ad0625

Environmental parameter estimation with the two-level atom probes

Mengmeng Luo(罗萌萌), Wenxiao Liu(刘文晓), Yuetao Chen(陈悦涛), Shangbin Han(韩尚斌), and Shaoyan Gao(高韶燕)
Chin. Phys. B, 2022, 31 (**5**): 050304. DOI: 10.1088/1674-1056/ac364f

Quantum speed limit for the maximum coherent state under the squeezed environment

Kang-Ying Du(杜康英), Ya-Jie Ma(马雅洁), Shao-Xiong Wu(武少雄), and Chang-Shui Yu(于长水)
Chin. Phys. B, 2021, 30 (**9**): 090308. DOI: 10.1088/1674-1056/ac0daf

---

Phase-matching enhanced quantum phase and amplitude estimation of a two-level system in a squeezed reservoir

Yan-Ling Li(李艳玲)[1], Cai-Hong Liao(廖彩红)[1], and Xing Xiao(肖兴)[2,†]

[1] *School of Information Engineering, Jiangxi University of Science and Technology, Ganzhou* 341000, *China*
[2] *College of Physics and Electronic Information, Gannan Normal University, Ganzhou* 341000, *China*

(Received 27 August 2024; revised manuscript received 24 October 2024; accepted manuscript online 7 November 2024)

Squeezed reservoir engineering is a powerful technique in quantum information that combines the features of squeezing and reservoir engineering to create and stabilize non-classical quantum states. In this paper, we focus on the previously neglected aspect of the impact of the squeezing phase on the precision of quantum phase and amplitude estimation based on a simple model of a two-level system (TLS) interacting with a squeezed reservoir. We derive the optimal squeezed phase-matching conditions for phase ϕ and amplitude θ parameters, which are crucial for enhancing the precision of quantum parameter estimation. The robustness of the squeezing-enhanced quantum Fisher information against departures from these conditions is examined, demonstrating that minor deviations from phase-matching can still result in remarkable precision of estimation. Additionally, we provide a geometric interpretation of the squeezed phase-matching conditions from the classical motion of a TLS on the Bloch sphere. Our research contributes to a deeper understanding of the operational requirements for employing squeezed reservoir engineering to advance quantum parameter estimation.

Keywords: quantum parameter estimation, squeezed reservoir, phase-matching conditions, quantum Fisher information

PACS: 03.67.–a, 03.65.Yz, 03.65.Aa

DOI: 10.1088/1674-1056/ad8f9e **CSTR:** 32038.14.CPB.ad8f9e

1. Introduction

Quantum parameter estimation is a critical area in quantum information science.[1,2] It serves as the foundation for the precise measurement of physical quantities, which is essential for a range of applications including quantum computing[3] and quantum sensing.[4] The importance of quantum parameter estimation lies in its potential to surpass classical limits of measurement precision, known as the standard quantum limit, by utilizing quantum phenomena such as entanglement and squeezing.[5] Recent developments have shown that quantum entanglement and squeezed states can be used to achieve measurement precisions that approach or even exceed the Heisenberg limit, which represents the ultimate quantum limit of precision.[6,7] Notwithstanding these advances, two significant challenges remain. One is the practical realization of highly entangled and squeezed states in a scalable manner because the greater the number of entangled particles, the larger the increase in precision. Fortunately, the entangled state of more than 10000 spin-1 atoms has been realized by employing the techniques of quantum phase transition.[8] The other is the mitigation of noise, since any realistic quantum system interacts with its surrounding environment leading to unwanted noise that significantly reduces the precision of quantum parameter estimation.[9] Overcoming environmental noise is essential for the continued development and implementation of quantum-enhanced technologies.

Over the past decade, researchers have put forth a number of techniques aimed at mitigating environmental noise and improving the precision of quantum parameter estimation. These methods include dynamical decoupling,[10,11] quantum error correction,[12,13] continuous non-demolition measurement[14] and the use of decoherence-free subspaces,[15,16] which collectively demonstrate advances and ongoing challenges in the field of quantum parameter estimation. However, these methods also have disadvantages that restrict their capabilities. For example, dynamical decoupling may be less effective against high-frequency noise or noise with a broad spectrum, while quantum error correction requires a significant overhead in terms of additional physical qubits and complex error-detection circuits. Squeezing is well-established as a mechanism that enhances atom–field coupling and surpasses traditional limits by improving the signal-to-noise ratio in measurement.[17,18] This capability is crucial for the advancement of quantum technologies, as it enables more precise qubit readouts and paves the way for innovative approaches to efficient quantum information processing.[19] The technology of squeezed reservoir engineering has gradually emerged in recent years as a means to counteract the detrimental effects of noise.[20–27] The essential concept is that the squeezed reservoir imprints its squeezing feature onto the quantum system, thereby enabling the latter to reduce quantum fluctuations in certain quadratures and enhance precision in the presence

†Corresponding author. E-mail: xiaoxing@gnnu.edu.cn

© 2025 Chinese Physical Society and IOP Publishing Ltd. All rights, including for text and data mining, AI training, and similar technologies, are reserved.

of environmental interactions. Squeezed reservoir engineering has been employed to maintain high levels of spin squeezing, generate stable entangled states[21–26] and enhance quantum phase synchronization.[30]

This manuscript delves into the utilization of squeezed reservoir engineering to enhance the precision of quantum parameter estimation. In contrast to prior investigations that primarily focussed on the relationship between the squeezing strength of the reservoir and quantum entanglement or spin squeezing,[20–29] our work underscores the significance of the squeezing phase of the reservoir in quantum parameter estimation. The phase-matching condition plays a pivotal role in quantum parameter estimation, providing the potential to surpass the standard quantum limit.[31–33] This condition facilitates the optimization of quantum Fisher information (QFI), which is essential for improving phase sensitivity in quantum metrology. In Ref. [32], Liu *et al*. discussed the phase-matching condition as a mechanism for enhancing sensitivity in a Mach–Zehnder interferometer when one of the inputs is in an odd/even state. Furthermore, the phase-matching condition was also investigated within the framework of squeezed-state interferometry, which incorporates finite photon-number resolution.[33] In Refs. [32,33], the phase-matching condition not only improved the sensitivity of phase measurements but also sustained this advantage in scenarios characterized by photon losses or restricted photon-number resolution at detectors. Such robustness makes the phase-matching condition indispensable for practical applications in quantum-enhanced sensing and metrology.

In this paper, we identify the optimal squeezed phase-matching conditions for the estimation of the parameters ϕ and θ in a two-level system (TLS) as $2\phi-\Phi=\pm\pi$ and $2\phi-\Phi=0$ or 2π, where Φ is the squeezing phase. Our analysis reveals that the enhancement of precision in quantum parameter estimation through squeezed reservoir engineering is contingent on meeting these squeezed phase-matching conditions; otherwise, it could potentially compromise the estimation precision. To this end, we also investigated the robustness of squeezing-enhanced quantum parameter estimation against deviations from the squeezed phase-matching conditions. Finally, by examining the classical motion of the TLS on the Bloch sphere, we present a geometric picture to illustrate the distinction between these two squeezed phase-matching conditions. This study contributes to a deeper understanding of the operational requirements for employing squeezed reservoir engineering in advancing quantum parameter estimation, thereby offering valuable insights for experimental realization.

2. Theoretical model

We consider a model of a TLS coupled to a squeezed reservoir. Note that our model is not limited to specific physical systems. An example is that a natural atom is embedded in a waveguide which acts as a squeezed reservoir when it is driven by a broadband squeezed field. In the interaction picture, the Hamiltonian is ($\hbar=1$)[34]

$$H_{\rm int}=\sigma_-(t)\mathcal{B}^\dagger(t)+\sigma_+(t)\mathcal{B}(t), \tag{1}$$

with TLS operators $\sigma_\pm(t)=\sigma_\pm\exp(\pm{\rm i}\omega_0 t)$ and a reservoir operator $\mathcal{B}(t)=\sum_k g_k b_k\exp(-{\rm i}\omega_k t)$. ω_0 is the transition frequency of the TLS, and g_k is the coupling strength. b_k is the annihilation operator of the kth mode of the reservoir with frequency ω_k.

The squeezed reservoir centered around the TLS transition frequency ω_0 is characterized by the bath correlation functions

$$\begin{aligned}
&\langle\mathcal{B}^\dagger(t)\mathcal{B}(t')\rangle=\gamma_0 N\delta(t-t'),\\
&\langle\mathcal{B}(t)\mathcal{B}^\dagger(t')\rangle=\gamma_0(N+1)\delta(t-t'),\\
&\langle\mathcal{B}(t)\mathcal{B}(t')\rangle=\gamma_0\chi\,{\rm e}^{-{\rm i}\Phi-2{\rm i}\omega_0 t}\delta(t-t'),\\
&\langle\mathcal{B}^\dagger(t)\mathcal{B}^\dagger(t')\rangle=\gamma_0\chi\,{\rm e}^{{\rm i}\Phi+2{\rm i}\omega_0 t}\delta(t-t'),
\end{aligned} \tag{2}$$

where γ_0 is the spontaneous emission rate of the TLS. $N=n\cosh 2r+\sinh^2 r$ is the effective photon number with $n=1/[\exp(\frac{\hbar\omega_k}{k_{\rm B}T})-1)]$. Here, T represents the temperature of the squeezed reservoir. $\chi=-(1/2)(2n+1)\sinh 2r$ is the squeezing parameter with r and Φ being the squeezing strength and phase.

With the previously mentioned correlation functions in mind, we can derive the master equation for the TLS under the Born–Markov approximation. The time evolution of the reduced density matrix operator for the TLS is described by

$$\begin{aligned}
\frac{{\rm d}\rho}{{\rm d}t}=&-\frac{\gamma_0(N+1)}{2}(\sigma_+\sigma_-\rho+\rho\sigma_+\sigma_--2\sigma_-\rho\sigma_+)\\
&-\frac{\gamma_0 N}{2}(\sigma_-\sigma_+\rho+\rho\sigma_-\sigma_+-2\sigma_+\rho\sigma_-)\\
&-\gamma_0\chi\,{\rm e}^{{\rm i}\Phi}\sigma_+\rho\sigma_+-\gamma_0\chi\,{\rm e}^{-{\rm i}\Phi}\sigma_-\rho\sigma_-.
\end{aligned} \tag{3}$$

We assume the initial state of the TLS to be a pure state

$$|\psi\rangle_{\rm in}=\cos\frac{\theta}{2}|g\rangle+{\rm e}^{{\rm i}\phi}\sin\frac{\theta}{2}|e\rangle, \tag{4}$$

where $0\le\theta\le\pi$ and $0\le\phi\le 2\pi$. The state at time t can be obtained by solving the master equation

$$\rho(t)=\begin{pmatrix}\rho_{ee} & \rho_{eg}\\ \rho_{ge} & \rho_{gg}\end{pmatrix}, \tag{5}$$

where

$$\begin{aligned}
\rho_{ee}&=\frac{N}{2N+1}+\left(\frac{1-\cos\theta}{2}-\frac{N}{2N+1}\right)d^2,\\
\rho_{eg}&=\frac{1}{2}d\sin\theta\,{\rm e}^{{\rm i}\phi}\left[\cosh(\chi\gamma_0 t)-\sinh(\chi\gamma_0 t)\,{\rm e}^{-{\rm i}(2\phi-\Phi)}\right],\\
\rho_{ge}&=\frac{1}{2}d\sin\theta\,{\rm e}^{-{\rm i}\phi}\left[\cosh(\chi\gamma_0 t)-\sinh(\chi\gamma_0 t)\,{\rm e}^{{\rm i}(2\phi-\Phi)}\right],
\end{aligned}$$

$$\rho_{gg} = \frac{N+1}{2N+1} - \left(\frac{1-\cos\theta}{2} - \frac{N}{2N+1}\right) d^2, \tag{6}$$

with $d = \mathrm{e}^{-(2N+1)\gamma_0 t/2}$.

This analytical expression allows us to estimate any parameter included in Eq. (4). According to the theory of quantum parameter estimation, the ultimate precision of estimating a parameter is limited by the quantum Cramér–Rao bound (QCRB)[35]

$$\Delta\hat{\vartheta} \geq \frac{1}{\sqrt{\nu F_\vartheta}}, \tag{7}$$

where ν is the number of repetitions and F_ϑ is the QFI. Calculation of the QFI typically requires solving the eigenvalues and eigenstates of the density matrix. Fortunately, for a single-qubit mixed state, Watanabe *et al*. proposed a method for directly calculating the QFI using the Bloch vector $\boldsymbol{m}$[36,37]

$$F_\vartheta = \begin{cases} |\partial_\vartheta \boldsymbol{m}|^2 + \frac{(\boldsymbol{m}\cdot\partial_\vartheta \boldsymbol{m})^2}{1-|\boldsymbol{m}|^2}, & \text{if } |\boldsymbol{m}| < 1, \\ |\partial_\vartheta \boldsymbol{m}|^2, & \text{if } |\boldsymbol{m}| = 1, \end{cases} \tag{8}$$

where $\boldsymbol{m} = (m_x, m_y, m_z)^{\mathrm{T}}$ satifies $\rho = (1/2)(1 + \boldsymbol{m}\cdot\hat{\boldsymbol{\sigma}})$. Note that this method can be generalized to calculate the quantum Fisher information matrix (QFIM) in the Bloch representation of a d-dimensional density matrix.[38]

3. Phase-matching enhanced quantum phase estimation

In this section, we discuss how to enhance the precision of the phase parameter ϕ through squeezed reservoir engineering. The QFI F_ϕ can be calculated as

$$F_\phi = d^2 \sin^2\theta (A+B) - \frac{d^4 \sin^4\theta \sinh^2(2\chi\gamma_0 t)\sin^2(2\phi-\Phi)}{4\rho_{ee}^2 - 4\rho_{ee} + d^2\sin^2\theta(A-B)}, \tag{9}$$

where $A = \cosh(2\chi\gamma_0 t)$ and $B = \sinh(2\chi\gamma_0 t)\cos(2\phi-\Phi)$.

The numerical results in Fig. 1 demonstrate the dynamic evolution of F_ϕ under varying reservoir temperatures and squeezing strengths. As expected, in the absence of squeezing, the interaction between the system and the thermal reservoir leads to a rapid decay of F_ϕ, as depicted in Fig. 1(a). Conversely, with the introduction of a squeezed reservoir, the decay of the QFI can be significantly mitigated. Figure 1(b) shows that the stronger the squeezing effect of the reservoir, the more pronounced the effect becomes. The underlying mechanism could be attributed to the fact that the squeezing reservoir transfers the squeezing characteristics to TLS, thereby diminishing the influence of environmental noise on TLS. This can be validated through the discussion in Eq. (11).

A more detailed analysis reveals that enhancement of the QFI is not only related to the squeezing strength but also to the squeezing phase Φ. Figure 2(a) illustrates that even under significant squeezing effects, if the squeezing phase is not chosen appropriately the enhancement of the QFI is actually less effective than in the case without squeezing. According to Eq. (9), we conjecture that the optimal squeezing phase should satisfy $\cos(2\phi-\Phi) = -1$ and $\sin(2\phi-\Phi) = 0$. This could be confirmed by solving the equations $\frac{\partial F_\phi}{\partial(2\phi-\Phi)} = 0$ and $\frac{\partial^2 F_\phi}{\partial(2\phi-\Phi)^2} < 0$. Then we can obtain that the squeezed phase-matching condition for F_ϕ is

$$2\phi - \Phi = \pm\pi. \tag{10}$$

Then Eq. (9) yields

$$F_\phi = \sin^2\theta \exp\left[-(2n+1)\,\mathrm{e}^{-2r}\gamma_0 t\right]. \tag{11}$$

It is evident that the squeezing parameter significantly influences the dynamical behavior of the QFI within the framework of the TLS. When $r = 0$, the QFI is entirely governed by thermal noise, exhibiting a rapid decay characterized by $\exp[-(2n+1)\gamma_0 t]$. In contrast, the introduction of a phase-matched squeezed reservoir mitigates the impact of thermal noise, leading to a modification in the decay rate of the QFI from $(2n+1)\gamma_0$ to $(2n+1)\,\mathrm{e}^{-2r}\gamma_0$.

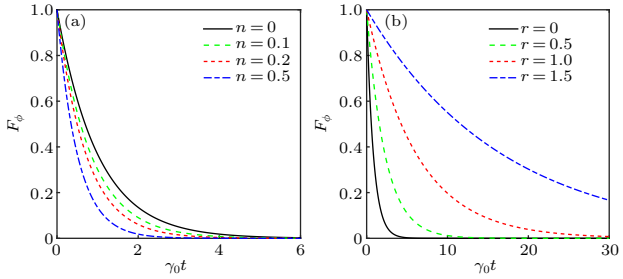


Fig. 1. The F_ϕ as a function of $\gamma_0 t$ with (a) $r = 0$ and (b) $n = 0.1$. The other parameters are $\theta = \pi/2$, $\phi = \pi/2$ and $\Phi = 0$.

In order to demonstrate the importance of squeezed phase-matching in enhancing the precision of phase parameter estimation, we introduce F_ϕ^{imp}

$$F_\phi^{\mathrm{imp}} = F_\phi - F_\phi(r=0), \tag{12}$$

which represents the improvement of QFI with squeezed reservoir engineering. The behavior of F_ϕ^{imp} as a function of r and $(2\phi-\Phi)$ is plotted in Fig. 2(b). It has been observed that the enhancement of QFI due to squeezing is notably pronounced in the vicinity where the squeezed phase-matching condition holds, for example $(2\phi-\Phi)/\pi = \pm 1$, while the blank regions indicate that the squeezed reservoir has not resulted in any enhancement if the phase-matching condition is not satisfied.

According to Eq. (9), it seems that the F_ϕ is dependent on the specific values of ϕ. It is natural to ask whether the achievable phase precision is consistent for different values of ϕ. Equation (11) indicates that when the squeezed phase-matching condition is satisfied, the achievable QFI is the same for any value of ϕ, and its precision improves with increasing

squeezing strength r, as shown in Fig. 2(c). It is well known that achieving perfect squeezed phase-matching is quite challenging. Consequently, an additional pertinent question arises: what is the resilience of the squeezing-enhanced F_ϕ with respect to the squeezed phase-matching condition? Figure 2(d) addresses this question. As shown in this figure, even when the squeezed phase-matching condition is not strictly met, such as $(2\phi-\Phi)\in[0.9\pi,1.1\pi]$, the estimated phase precision remains very good. The range of phase-matching error is entirely achievable in practice. For instance, in Refs. [39–42], the authors were able to control the phase deviation of the squeezed light to within 1.5 mrad through an ultra-low residual amplitude modulation control loop for the lengths and relative phase stabilizations of the degenerate optical parametric amplifiers.

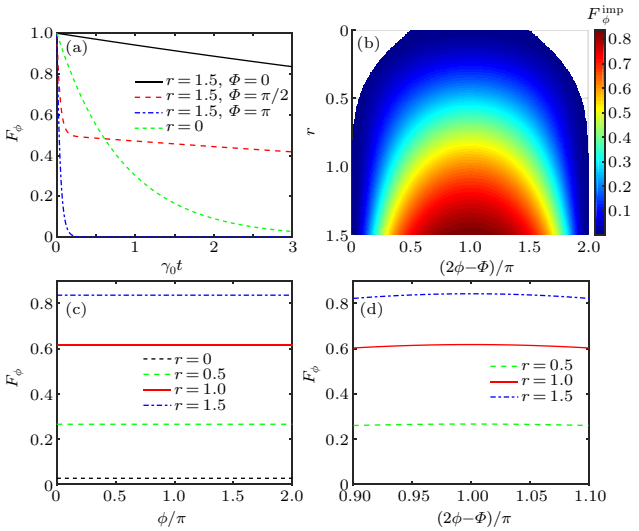


Fig. 2. The behaviors of F_ϕ in different cases: (a) F_ϕ as a function of $\gamma_0 t$ for different squeezing phases Φ; (b) $F_\phi^{\rm imp}$ as a function of r and $(2\phi-\Phi)$ at $\gamma_0 t=3$; (c) F_ϕ as a function of ϕ at $\gamma_0 t=3$ on the squeezed phase-matching condition (Eq. (10)); (d) F_ϕ as a function of the deviation from squeezed phase-matching condition at $\gamma_0 t=3$. The other parameters are $\theta=\pi/2$ and $n=0.1$.

4. Phase-matching enhanced quantum amplitude estimation

In this section, we consider estimation of the amplitude parameter θ. The QFI F_θ boils down to

$$F_\theta = d^2\cos^2\theta(A-B)+d^4\sin^2\theta - \frac{d^4\sin^2\theta[\cos\theta(A-B)-2\rho_{ee}+1]^2}{4\rho_{ee}^2-4\rho_{ee}+d^2\sin^2\theta(A-B)}. \tag{13}$$

The expression for F_θ is rather intricate and lacks informativeness. For a better understanding of how squeezing strength r and phase Φ affect the precision of amplitude parameter estimation, we present some numerical results in Fig. 3. Figure 3(a) first confirms that, under the condition of selecting an appropriate squeezing phase, the squeezed reservoir is beneficial for enhancing F_θ. To find the optimal squeezing phase, we similarly derived the phase-matching condition for the amplitude parameter by solving the equations $\frac{\partial F_\theta}{\partial(2\phi-\Phi)}=0$ and $\frac{\partial^2 F_\theta}{\partial(2\phi-\Phi)^2}<0$. The squeezed phase-matching condition for F_θ is

$$2\phi-\Phi=0 \text{ or } 2\pi. \tag{14}$$

When the phase-matching condition (14) is satisfied, F_θ can be approximated as (neglecting the fourth-order term of d)

$$F_\theta \approx \cos^2\theta\exp\left[-(2n+1)\,\mathrm{e}^{-2r}\gamma_0 t\right]. \tag{15}$$

We once again observe that the phase-matched squeezed reservoir affects F_θ by reducing the decay rate to $(2n+1)\,\mathrm{e}^{-2r}\gamma_0$. Figure 3(b) illustrates the variation of $F_\theta^{\rm imp}$ with respect to r and $(2\phi-\Phi)/\pi$. It can be observed that when the squeezed phase-matching condition is satisfied, an increase in squeezing can significantly enhance the precision of amplitude estimation.

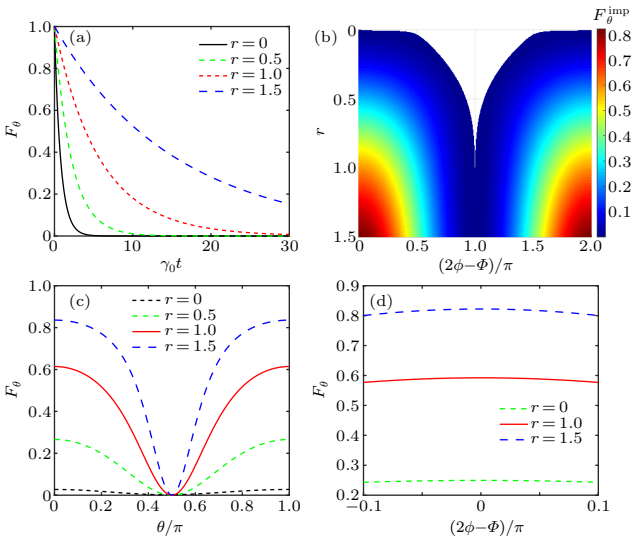


Fig. 3. The behaviors of F_θ in different cases: (a) F_θ as a function of $\gamma_0 t$ for different squeezing strengths r with $\theta=0.1\pi$ and $2\phi-\Phi=0$; (b) $F_\theta^{\rm imp}$ as a function of r and $(2\phi-\Phi)$ with $\theta=0.1\pi$ at $\gamma_0 t=3$; (c) F_θ as a function of θ at $\gamma_0 t=3$ on the squeezed phase-matching condition (Eq. (14)); (d) F_θ as a function of the deviation from squeezed phase-matching condition with $\theta=0.1\pi$ at $\gamma_0 t=3$. The other parameter is $n=0.1$.

Similarly, F_θ also depends on the specific value of θ. Therefore, it is necessary to discuss whether the estimation precision is the same for any θ when the squeezed phase-matching condition is satisfied. As can be seen from Fig. 3(c), the answer is negative, which is different from the results in Fig. 2(c) where the achievable F_ϕ is the same for any ϕ. This could be explained as follows. The amplitude parameter θ is a parameter related to the populations of the excited and ground states. Its estimation precision primarily depends on the population difference between the excited state and the ground state. When the population difference between the excited state and the ground state is at its maximum ($\theta=0$ or π), the estimation precision is highest, and vice versa. If the populations of the excited state and the ground state are

equal it indicates that the system is in an equal superposition state ($\theta = \pi/2$), and the estimation precision for the parameter θ is at its lowest. Fortunately, the squeezing-enhanced F_θ is robust against deviation from the squeezed phase-matching condition, as shown in Fig. 3(d).

5. Geometric picture of the squeezed phase-matching conditions

Understanding the different squeezed phase-matching conditions required to estimate parameters ϕ and θ is not an easy task since QFI is a relatively subtle concept. In this study, we endeavor to understand this by tracking the 'classical motion' of the TLS in phase space. In order to obtain the 'classical trajectories', we choose the coherent-spin state representation $\{|\theta,\phi\rangle\}$ and use the approximation $\langle\sigma_i\rangle = \mathrm{Tr}(\sigma_i|\theta,\phi\rangle\langle\theta,\phi|)$ with $i = x,y,z$. Subsequently, we can deduce the following relationships:[43]

$$\langle\sigma_x\rangle \to \langle\sin\theta\cos\phi\rangle, \quad \langle\sigma_y\rangle \to \langle-\sin\theta\sin\phi\rangle,$$
$$\langle\sigma_z\rangle \to \langle\cos\theta\rangle. \tag{16}$$

This indicates that one can obtain the dynamical evolutions of θ and ϕ from the dynamical equations of the Pauli operators. The dynamical equations of the Pauli operators in the Heisenberg picture are written as

$$\frac{\mathrm{d}\langle\sigma_x\rangle}{\mathrm{d}t} = (\omega_0 - \gamma_0\chi\sin\Phi)\sin\phi\sin\theta - \gamma_0\left[\frac{1}{2}(2N+1) + \chi\cos\Phi\right]\cos\phi\sin\theta, \tag{17}$$

$$\frac{\mathrm{d}\langle\sigma_y\rangle}{\mathrm{d}t} = (\omega_0 + \gamma_0\chi\sin\Phi)\cos\phi\sin\theta + \gamma_0\left[\frac{1}{2}(2N+1) - \chi\cos\Phi\right]\sin\phi\sin\theta, \tag{18}$$

$$\frac{\mathrm{d}\langle\sigma_z\rangle}{\mathrm{d}t} = -\gamma_0 - \gamma_0(2N+1)\cos\theta. \tag{19}$$

With the relations (16) in mind, it is easy to find that the time evolutions of θ and ϕ are determined by

$$\frac{\mathrm{d}\theta}{\mathrm{d}t} = \gamma_0\csc\theta + \gamma_0(2N+1)\cot\theta, \tag{20}$$

$$\frac{\mathrm{d}\phi}{\mathrm{d}t} = -\omega_0 + \gamma_0\chi\sin(2\phi - \Phi). \tag{21}$$

When given the initial values of θ and ϕ, we can plot the 'classical trajectories' of the TLS on the Bloch sphere, as shown in Fig. 4. It is important to clarify that Fig. 4 does not represent the evolution trajectory of the TLS governed by the master equation; rather, it illustrates the 'classical motion' of a qubit within phase space, derived from Eqs. (20) and (21). Intuitively, this process can be likened to tracking the directional coordinates (azimuthal angle ϕ and polar angle θ) of a classical spin. Consequently, the Bloch vector remains normalized and is consistently projected onto the surface of the Bloch sphere throughout its evolution. Based on these 'classical trajectories', we attempt to understand the difference between two squeezed phase-matching conditions from a geometric perspective.

Preceding this analysis, it is imperative to furnish supplementary elucidation regarding the physical intuition behind QFI. The QCRB indicates that a greater QFI corresponds to enhanced precision in parameter estimation. Nonetheless, an alternative interpretation of QFI can be obtained from its connection to Uhlmann fidelity[44,45]

$$F_\vartheta = \lim_{\varepsilon\to 0}\frac{8\,(1 - f\,[\rho(\vartheta),\rho(\vartheta+\varepsilon)])}{\varepsilon^2}, \tag{22}$$

where $f\,[\rho(\vartheta),\rho(\vartheta+\varepsilon)] = [\mathrm{Tr}\sqrt{\sqrt{\rho(\vartheta)}\rho(\vartheta+\varepsilon)\sqrt{\rho(\vartheta)}}]^2$. It is noteworthy that the Uhlmann fidelity quantifies the closeness or similarity between two quantum states. An Uhlmann fidelity of 1 indicates that the states are identical (fully overlapped), whereas a fidelity of 0 denotes that the states are orthogonal (completely distinguishable). Equation (22) demonstrates that the QFI is equivalent to the capability of distinguishing two adjacent states.

In Section 3, we demonstrated that the squeezed phase-matching condition for enhancing the phase precision F_ϕ is determined by the relation $2\phi - \Phi = \pm\pi$. In scenarios where the squeezed phase is not matched, such as $2\phi - \Phi = 0$, the value of F_ϕ will be reduced. As is well established, Fisher information quantifies the sensitivity of an observable quantity to infinitesimal variations in a parameter.[46] For example, given a measurement of the observable $\hat{M}$ whose outcomes depend on a parameter ϕ, the associated error can be expressed as $\delta\phi = \Delta\hat{M}/|\partial_\phi\langle\hat{M}\rangle|$ with $\partial_\phi = \partial/\partial\phi$ and $\langle\hat{M}\rangle$ an average value. From a geometric perspective, the denominator $|\partial_\phi\langle\hat{M}\rangle|$ represents the slope of $\langle\hat{M}\rangle$ with respect to ϕ. A steeper tangent at this point indicates a more precise estimation of the parameter ϕ. The QFI serves as a direct generalization of the classical Fisher information, thereby retaining a similar geometric interpretation. From this observation, we can infer that when squeezed phase-matching is satisfied, the squeezed reservoir will make the 'classical trajectory' of TLS on the Bloch sphere more sensitive to the azimuthal angle ϕ.

These physical insights can be validated through numerical simulations, as shown in Fig. 4. Specifically, in comparison to the scenario without a squeezed reservoir represented by the green line in Fig. 4(a), the slope of the curve corresponding to the estimation of parameter ϕ will be steeper under the condition of phase-matched squeezing, as shown by the blue line in Fig. 4(a). Consequently, the precision of estimating the parameter ϕ will be higher, whereby even minor changes in ϕ will lead to a significant deviation. This leads to an increased distinguishability between adjacent quantum states,

corresponding to lower Uhlmann fidelity and higher QFI. Conversely, if the squeezed phase-matching condition is not met, the squeezed reservoir will make the curve on the Bloch sphere very insensitive to changes in azimuthal angle. In this context, as depicted by the red line in Fig. 4(a), the slope of that curve corresponding to parameter ϕ diminishes. This insensitivity results in difficulties in distinguishing between adjacent quantum states, which corresponds to higher Uhlmann fidelity and reduced QFI.

A similar interpretation could be used to understand the squeezed phase-matching condition ($2\phi - \Phi = 0$ or 2π) in order to enhance the amplitude precision F_θ. A squeezed phase-matching reservoir drives the classical motion of the TLS along the longitude direction, rendering it highly sensitive to variations in the polar angle θ, as shown by the red line in Fig. 4(b). On the contrary, the squeezed reservoir with phase mismatch makes the curve less sensitive to the polar angle, as shown by the blue line in Fig. 4(b).

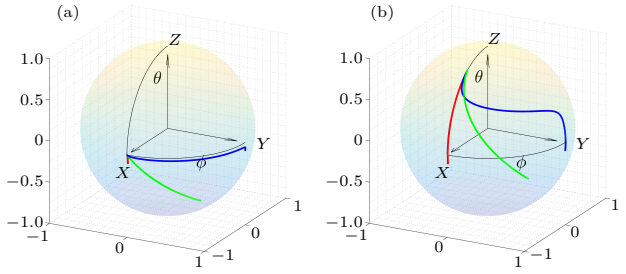


Fig. 4. The 'classical trajectories' of the TLS on the phase-matching and phase-mismatching conditions. (a) An illustration of the trajectories for estimating the phase with the initial parameters $\theta = \pi/2$ and $\phi = \pi/2$. The three curves respectively represent the cases with a phase-matching squeezed reservoir (blue line, $r = 1.5$ and $2\phi - \Phi = \pi$), a phase-mismatching squeezed reservoir (red line, $r = 1.5$ and $2\phi - \Phi = 0$) and without a squeezed reservoir (green line, $r = 0$). (b) An illustration of the trajectories for estimating the amplitude with the initial parameters $\theta = \pi/10$ and $\phi = \pi/2$. The three curves respectively represent the cases with a phase-matching squeezed reservoir (red line, $r = 1.5$ and $2\phi - \Phi = 0$), a phase-mismatching squeezed reservoir (blue line, $r = 1.5$ and $2\phi - \Phi = \pi$) and without a squeezed reservoir (green line, $r = 0$).

6. Discussion and conclusion

Before concluding, we would like to address the feasibility of implementing the squeezed phase-matching conditions. In the experiment, the squeezing phase is determined by the relative phase between the pump light and a coherent control field (CCF).[47] Initially, a CCF with a frequency shift of $+\Omega$ relative to the carrier frequency ω_0 is generated using a frequency-shifting device. Following its passage through an optical parametric oscillator (OPO) cavity, the quadratures of the CCF undergo parametric amplification and deamplification, resulting in the generation of upper-sideband $(\omega_0 + \Omega)$ and lower-sideband $(\omega_0 - \Omega)$ optical fields. A single photodetector can be employed to measure the photocurrent output from the OPO cavity. The photocurrent is determined by a factor $\cos(2\Omega t + 2\Phi)$. A demodulated signal at a frequency of 2Ω can be utilized to extract the error signal. By feeding back the error signal to a piezoelectric transducer (PZT)-mounted mirror in the path of the pump light, a stable squeezing phase Φ was locked.[48,49] In order to modulate the squeezing phase on demand, one can use electro-optic modulators to dynamically control the phase of the CCF relative to the pump light, allowing real-time adjustment of the squeezed phase-matching conditions.

In summary, we have explored the role of squeezed reservoir engineering in enhancing the precision of quantum phase and amplitude estimation, focusing on the previously neglected aspect of the impact of the squeezed phase on the precision of quantum phase and amplitude estimation using a simplistic model of a TLS coupled to a squeezed reservoir. We found that the squeezing angle plays a decisive role in these estimation processes. We demonstrated that the squeezed reservoir can significantly enhance the precision of the phase parameter on the squeezed phase-matching condition $2\phi - \Phi = \pm\pi$ and improve the precision of the amplitude parameter upon meeting the squeezed phase-matching condition $2\phi - \Phi = 0$ or 2π. Furthermore, we discussed the robustness of the squeezing-enhanced QFI against deviations from the optimal phase-matching conditions, finding that the estimation precision remains high even with moderate mismatches. To understand why the phase-matching conditions required for estimating ϕ and θ differ, we provided a geometric interpretation based on the classical motion of the TLS on the Bloch sphere. We observed that the fulfillment of the squeezed phase-matching condition $2\phi - \Phi = \pm\pi$ leads to the squeezed reservoir steering the classical motion of the TLS along the latitudinal direction, which is conducive to estimating the phase parameter ϕ. Conversely, upon satisfying the squeezed phase-matching condition $2\phi - \Phi = 0$ or 2π, the squeezed reservoir drives the classical motion of the TLS to evolve along the longitudinal direction, resulting in an increased sensitivity to the amplitude parameter θ. Our study advances the understanding of the operational prerequisites for employing squeezed reservoir engineering to enhance quantum parameter estimation, providing valuable insights for the utilization of squeezed reservoir engineering in diverse quantum information technologies.

Acknowledgments

Project supported by the National Natural Science Foundation of China (Grant No. 12265004), Jiangxi Provincial Natural Science Foundation (Grant No. 20242BAB26010), the National Natural Science Foundation of China (Grant No. 12365003), and Jiangxi Provincial Natural Science Foundation (Grant Nos. 20212ACB211004 and 20212BAB201014).

References

[1] Giovannetti V, Lloyd S and Maccone L 2011 *Nat. Photonics* **5** 222
[2] Tóth G and Apellaniz I 2014 *J. Phys. A: Math. Theor.* **47** 424006
[3] Demkowicz-Dobrzański R and Markiewicz M 2015 *Phys. Rev. A* **91** 062322
[4] Taylor M A and Bowen W P 2016 *Phys. Rep.* **615** 1
[5] Giovannetti V, Lloyd S and Maccone L 2004 *Science* **306** 1330
[6] Zwierz M, Pérez-Delgado C A and Kok P 2012 *Phys. Rev. A* **85** 042112
[7] Demkowicz-Dobrzański R, Kołodyński J and Guţă M 2012 *Nat. Commun.* **3** 1063
[8] Zou Y Q, Wu L N, Liu Q, Luo X Y, Guo S F, Cao J H, Tey M K and You L 2018 *Proc. Natl. Acad. Sci. USA* **115** 6381
[9] Degen C L, Reinhard F and Cappellaro P 2017 *Rev. Mod. Phys.* **89** 035002
[10] de Lange G, Wang Z H, Ristè D, Dobrovitski V V and Hanson R 2010 *Science* **330** 60
[11] Zhang J, Du P, Jing L, Xu P, You L and Zhang W 2024 *Chin. Phys. B* **33** 030301
[12] Kessler E M, Lovchinsky I, Sushkov A O and Lukin M D 2014 *Phys. Rev. Lett.* **112** 150802
[13] Hong H Y, Lu X J and Kuang S 2023 *Chin. Phys. B* **32** 040603
[14] Rossi M A C, Albarelli F, Tamascelli D and Genoni M G 2020 *Phys. Rev. Lett.* **125** 200505
[15] Zhang C, Yu P, Jadbabaie A and Hutzler N R 2023 *Phys. Rev. Lett.* **131** 193602
[16] Hamann A, Sekatski P and Dür W 2022 *Quantum Sci. Technol.* **7** 025003
[17] Qin W, Miranowicz A, Li P B, Lü X Y, You J Q and Nori F 2018 *Phys. Rev. Lett.* **120** 093601
[18] Qin W, Miranowicz A and Nori F 2022 *Phys. Rev. Lett.* **129** 123602
[19] Qin W, Kockum A F, Muñoz C S, Miranowicz A and Nori F 2024 *Phys. Rep.* **1078** 1
[20] Kienzler D, Lo H Y, Keitch B, De Clercq L, Leupold F, Lindenfelser F, Marinelli M, Negnevitsky V and Home J P 2015 *Science* **347** 53
[21] Yang C J, An J H, Yang W and Li Y 2015 *Phys. Rev. A* **92** 062311
[22] Hu X, Hu Q, Li L, Huang C and Rao S 2017 *Phys. Rev. A* **96** 063824
[23] Groszkowski P, Koppenhöfer M, Lau H K and Clerk A A 2022 *Phys. Rev. X* **12** 011015
[24] Bai S Y and An J H 2021 *Phys. Rev. Lett.* **127** 083602
[25] Hou Q Z, You J B, An J H, Yang W L, Cheng C Y and Feng M 2018 *Opt. Express* **26** 20459
[26] Hou Q Z, Yang C J, Chen C Y, An J H, Yang W L and Feng M 2019 *Phys. Rev. A* **100** 032302
[27] Mendonça T M, Souza A M, de Assis R J, de Almeida N G, Sarthour R S, Oliveira I S and Villas-Boas C J 2020 *Phys. Rev. Res.* **2** 043419
[28] Maleki Y and Ahansaz B 2020 *Phys. Rev. A* **102** 020402
[29] Lu X, Cao W, Yi W, Shen H and Xiao Y 2021 *Phys. Rev. Lett.* **126** 223603
[30] Xiao X, Lu T X, Zhong W J and Li Y L 2024 arXiv:2408.09850
[31] Caves C M 1981 *Phys. Rev. D* **23** 1693
[32] Liu J, Jing X and Wang X 2013 *Phys. Rev. A* **88** 042316
[33] Liu P, Wang P, Yang W, Jin G R and Sun C P 2017 *Phys. Rev. A* **95** 023824
[34] Breuer H P and Petruccione F 2002 *The theory of open quantum systems* (Oxford: Oxford University Press)
[35] Helstrom C W 1969 *J. Stat. Phys.* **1** 231
[36] Watanabe Y, Sagawa T and Ueda M 2010 *Phys. Rev. Lett.* **104** 020401
[37] Watanabe Y, Sagawa T and Ueda M 2011 *Phys. Rev. A* **84** 042121
[38] Liu J, Yuan H, Lu X M and Wang X 2020 *J. Phys. A: Math. Theor.* **53** 023001
[39] Li Z X, Ma W G, Yang W H , Wang Y J and Zheng Y H 2016 *Opt. Lett.* **41** 3331
[40] Li Z X, Tian Y H, Wang Y J, Ma W G and Zheng Y H 2019 *Opt. Express* **27** 7064
[41] Yang W H, Shi S P, Wang Y J, Ma W G, Zheng Y H and Peng K C 2017 *Opt. Lett.* **42** 4553
[42] Zhang W, Jiao N, Li R, Tian L, Wang Y and Zheng Y 2021 *Opt. Express* **29** 24315
[43] Zhang L, Wang Z, Wang Y, Zhang J, Wu Z, Jie J and Lu Y 2023 *Phys. Rev. Res.* **5** 033209
[44] Braunstein S L and Caves C M 1994 *Phys. Rev. Lett.* **72** 3439
[45] Šafránek D 2017 *Phys. Rev. A* **95** 052320
[46] Sidhu J S and Kok P 2020 *AVS Quantum Sci.* **2** 014701
[47] Schnabel R 2017 *Phys. Rep.* **684** 1
[48] Chelkowski S, Vahlbruch H, Hage B, Franzen A, Lastzka N, Danzmann K and Schnabel R 2005 *Phys. Rev. A* **71** 013806
[49] Vahlbruch H, Chelkowski S, Hage B, Franzen A, Danzmann K and Schnabel R 2006 *Phys. Rev. Lett* **97** 011101